IFAI Geosynthetics Conference
Feb. 10-13, 2019 | Houston, TX USA

In-Isolation Properties of Biaxial and Triangular Geogrids along Various Directions

M. M. Aboelwafa, M.Sc.,[1] G. H. Roodi, Ph.D., and J. G. Zornberg, Ph.D., P.E.

[1]Department of Civil, Architectural, and Environmental Engineering, The University of Texas at Austin, 301 E. Dean Keeton St. Stop C1792, Austin, TX 78712; e-mail: m.aboelwafa@aun.edu.eg

ABSTRACT

With the advent of triangular aperture geogrids, questions have been raised regarding properties of these products (as well as traditional biaxial geogrids) along various directions. This study presents the results of an experimental program conducted to determine in-isolation properties of geosynthetic in various directions. Specifically, wide-width tensile tests were conducted using two geosynthetic products including a triangular aperture geogrid and a biaxial geogrid. The geosynthetic specimens were cut in five directions including machine direction, cross-machine direction, and at orientations of 30, 45, and 60 degrees between the machine and cross-machine directions. Ultimate tensile strength and tensile stiffness of geosynthetic specimens at 0.5, 1, and 2 % strains were obtained from wide-width tensile tests. Overall, it was found that the geosynthetic ultimate tensile strength and in-isolation stiffness were reasonably isotropic in the triangular aperture geogrid. However, in the biaxial geogrid these properties were found to be significantly different in the machine and cross-machine directions as compared to the other directions. Based on the experimental results, empirical equations were derived to estimate the ultimate tensile strength and tensile stiffness along an arbitrary angle. Predictions obtained using the developed empirical equations in this study were then compared to the experimental data reported in other original studies and a reasonably good agreement was found.

INTRODUCTION

Geogrids are polymeric materials (e.g., polyester, polypropylene, polyethylene) which are manufactured using various manufacturing techniques such as knitting, welding, or extruded and punched-drawn (Koerner 2012). Geogrids with rectangular or square apertures have been manufactured to carry tensile forces mainly in one or two directions (i.e., along their machine and/or cross-machine ribs). These geogrids have been referred to as (1) uniaxial geogrids, when they are manufactured to perform mainly in one-direction (e.g., in reinforcement of walls and slopes (e.g., Han and Leshchincky 2010), or (2) biaxial geogrids, when they are manufactured to perform in two directions (e.g., in stabilization of roads and foundations (e.g., Abu-Farsakh et al. 2008). A more recent class of geogrids, referred to as triaxial or triangular geogrids, are manufactured with triangular apertures. These geogrids are aimed at providing similar properties along all directions and have been suggested for conditions that the geogrid is subjected to multi-directional loads. The triangular geogrids are expected to provide comparatively more isotropic stiffness properties than biaxial geogrids and thus perform comparatively better under loading conditions where multi-directional loads are applied. However, potential benefits of triangular

geogrids in providing more isotropic properties than biaxial geogrids need to be investigated in unconfined and confined conditions.

Several researchers have studied the use of biaxial geogrids in different application such as subgrade improvement, unbound base stabilization, and foundation reinforcement (e.g., Helstrom et al. 2006; Brown et al. 2007; Abdullah and Edil 2007; Tang et al. 2008). In real applications, the load distribution may not necessarily follow the orientations of the machine and cross-machine ribs (e.g., under traffic loads); therefore, questions have been raised regarding properties of biaxial (as well as triangular) geogrids along directions different from the orientations of the geogrid ribs. Dong et al. (2010) conducted a numerical study, by using the numerical software FLAC, to investigate the effect of geogrid orientation on the tensile strength and tensile stiffness under uniaxial loading for triangular and biaxial geogrids. Dong et al. (2010) found an anisotropic ultimate tensile strength and stiffness for the biaxial geogrid with significantly high tensile strength and stiffness along machine and cross-machine directions and particularly low strength and stiffness along other directions. However, they found a comparatively uniform tensile strength along all directions for triangular geogrids. Also, Swan and Yuan (2013) developed a theoretical approach to determine the tensile strength of a triangular geogrid based on the single-rib tensile properties and they found that the triangular geogrid had a uniform tensile strength along all directions. However, limited experimental research has been carried out to measure the in-isolation properties of geosynthetics using representative specimens of these products.

This study focuses on experimental evaluation of the impact of geosynthetic orientation on in-isolation geosynthetic properties for triangular and biaxial geogrids. Specifically, wide-width tensile tests were conducted along various directions of a triangular geogrid and a biaxial geogrid and the obtained results were used to gain a better understanding on the tensile properties of the geosynthetics, including ultimate tensile strength and tensile stiffness, along different directions. Experimental data was used to develop empirical equations to estimate in-isolation properties of triangular and biaxial geogrids along an arbitrary angle based on the properties obtained in the machine and cross-machine directions. Predictions from the developed empirical equations were compared to the experimental data reported in other original studies.

MATERIALS AND EXPERIMENTAL SETUP

A biaxial and triangular geogrid that were formed integrally from punched and drawn polypropylene sheets were used in this study (Figures 1(a) and 1(b)). Specifications of the geogrids reported by the manufacturer is presented in Table 1. In this study, the triangular geogrid is referred to as GGT and the biaxial geogrid is referred to as GGB.

(a) 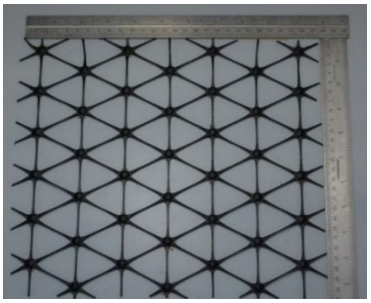 **(b)** 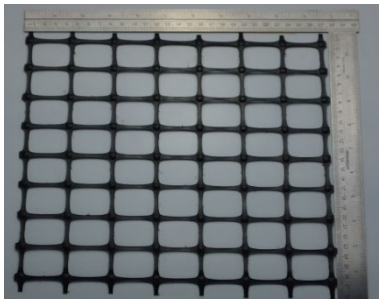

Figure 1. Geogrids used in this study: (a) triaxial or triangular (GGT); (b) biaxial (GGB).

The wide-width tensile tests were conducted according to the procedure outlined in ASTM D6637 (2015). This standard allows three types of test specimens including: (1) single-rib specimens (2) multi-rib specimens with a minimum width of 200 mm, and (3) multi-layered specimens. The wide-width tensile tests were carried out at a constant strain rate of 10 % per min on specimens of dimensions 200 mm x 200 mm. The tests were conducted using a conventional loading frame and a fabricated flat jaw grip system on top and a vise in the bottom. Strains were measured using image analysis technique using a digital camera mounted onto a horizontal frame installed in front of the specimens. The main steps of the testing procedure are shown in Figure 2.

Table 1. Manufacturer specifications of geogrids used in this study.

Property	GGT	GGB
Geosynthetic type	Triangular Geogrid	Biaxial Geogrid
polymer type	Polypropylene	Polypropylene
Manufacturing Process	Integrally-formed punched and drawn	Integrally-formed punched and drawn
Ultimate Tensile Strength, lbs/ft (kN/m) a. Machine Direction b. Cross-machine Direction	No data	850 (12.4) 1,300 (19)
Secant Tensile Stiffness at 1% strain, lbs/ft (kN/m) a. Machine Direction b. Cross-machine Direction	20,580 (300) 20,581 (300)	17,140 (250) 27,420 (400)
Secant Tensile Stiffness at 2% strain, lbs/ft (kN/m) a. Machine Direction b. Cross-machine Direction	No data	14,000 (205) 22,500 (330)
Secant Tensile Stiffness at 5% strain, lbs/ft (kN/m) a. Machine Direction b. Cross-machine Direction	No data	11,600 (170) 18,400 (270)

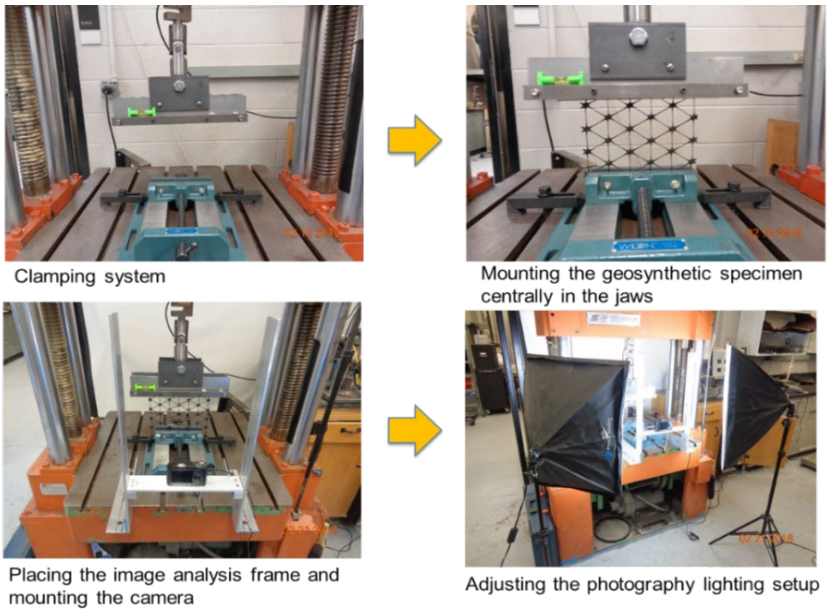

Figure 2. Main steps of wide-width tensile testing procedures.

EXPERIMENTAL RESULTS

The experimental results were used to estimate the ultimate tensile strength and the tensile stiffness for the two geogrids along the tested directions. The results along various directions are presented using a 360˚ radar chart. Specifically, the value presented at 0˚ angle corresponds to the geosynthetic mechanical property obtained along the cross-machine direction (CD) and the value presented at 90˚ angle corresponds to the geosynthetic mechanical property obtained along the machine direction (MD). The geosynthetic mechanical properties obtained along 30˚, 45˚, and 60˚ directions (measured from CD in counterclockwise direction), are then presented at 30˚, 45˚, and 60˚ angles, respectively.

Unit Tension-Tensile Strain Relationship. Tensile tests are performed to evaluate in-plane properties of geosynthetics in-isolation. In this test, a tensile load is applied along the longitudinal axis of the engaged length. The applied load and the resulting elongation of the specimen are measured. This data may then be converted to unit tension and strains to provide a direct indication of the material behavior. Figures 3 and 4 show the unit tension versus tensile strain plots for the triangular and biaxial geogrids, respectively.

Ultimate Tensile Strength. In this section the ultimate tensile strength is discussed for each product. The ultimate tensile strength, expressed in unit tension (kN/m), was obtained by dividing the maximum tensile load by the total width of the geosynthetic. Figure 5 shows that the ultimate wide-width tensile strength for the triangular geogrid is relatively uniform along all the tested directions. Specifically, the ultimate wide-width tensile strength for the triangular geogrid along various directions was found to range approximately from 17 to 21 kN/m.

Figure 5 also shows that the ultimate wide-width tensile strength for the biaxial geogrid highly depends on the direction of loading. When the tensile load was applied along the rib orientations (i.e., either the machine or cross-machine directions), the ultimate wide-width tensile strength was noticeably high. However, when the tensile load was applied along other directions (30˚, 45˚, and 60˚), the ultimate wide-width tensile strength was significantly lower. The reason for the reduced ultimate tensile strength in 30˚, 45˚, and 60˚ directions compared to the machine and the cross-machine directions can be attributed to potential bending and buckling of the geogrid ribs under compression. Unlike loading in the machine or cross-machine directions in which the tensile load is transferred directly through the ribs oriented along the loading direction, loading in other directions results in a complex load transfer mechanism in which a significant portion of geogrid ribs will be subjected to bending and compression. Because the slender geogrid ribs are not designed to have a strong resistance against compression and bending, they will fail at comparatively smaller load as compared to a tensile loading condition. Failure of those ribs subjected to compression and bending have probably resulted the significantly lower overall tensile resistance of the specimen in 30˚, 45˚, and 60˚ directions.

As shown in Figure 5, the ultimate tensile strength obtained for the biaxial geogrid from the experimental results was reasonably close to the ultimate tensile strength reported by the manufacturer specification along the machine and cross-machine directions.

In-Isolation Stiffness. In-isolation tensile stiffness of the geogrids, expressed as *J*, was obtained at 0.5 %, 1 %, and 2 % strains and compared between the two geogrids. As shown in Figures 6(a) to 6(c), the tensile stiffness for the biaxial geogrid was found to be higher than the triangular

geogrid in the machine and cross-machine directions. However, the tensile stiffness of the triangular geogrid was significantly higher than the biaxial geogrid along the other directions (i.e., 30˚, 45˚, and 60˚). Evaluation of the data presented in Figures 6(a) to 6(c) indicates that the tensile stiffness of the triangular geogrid at different strain levels were comparatively uniform along all tested directions. This finding suggests that the triangular geogrids may provide a comparatively isotropic in-plane mechanical response under different loading conditions.

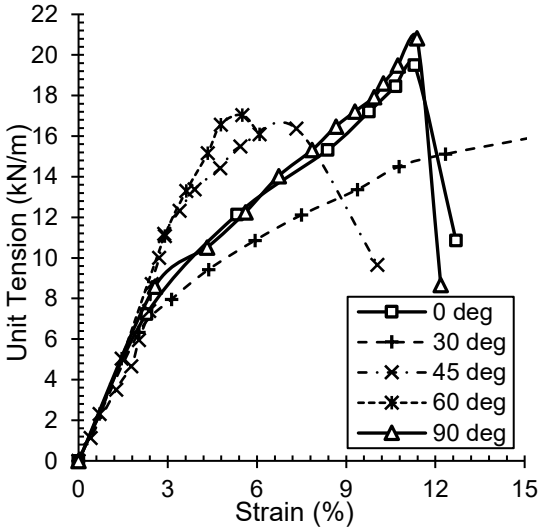

Figure 3. Unit tension-tensile strain data for the triangular geogrid.

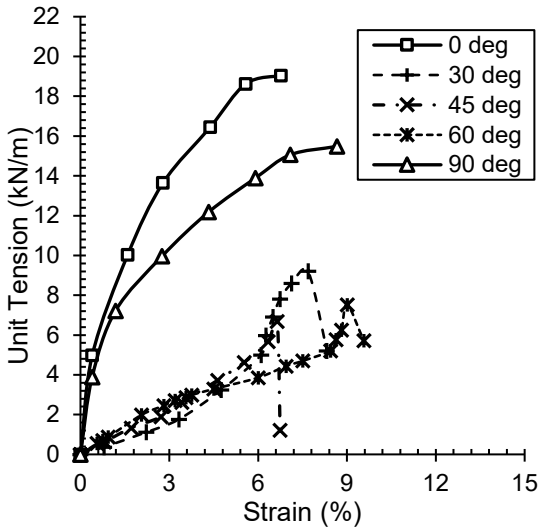

Figure 4. Unit tension-tensile strain data for the biaxial geogrid.

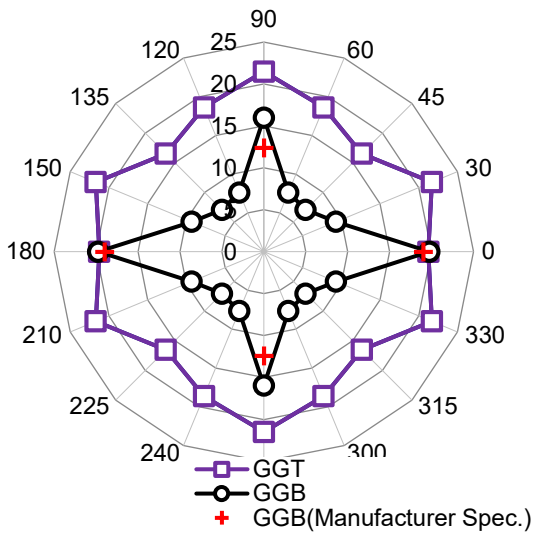

Figure 5. Ultimate wide-width tensile strength for geogrids (unit: kN/m).

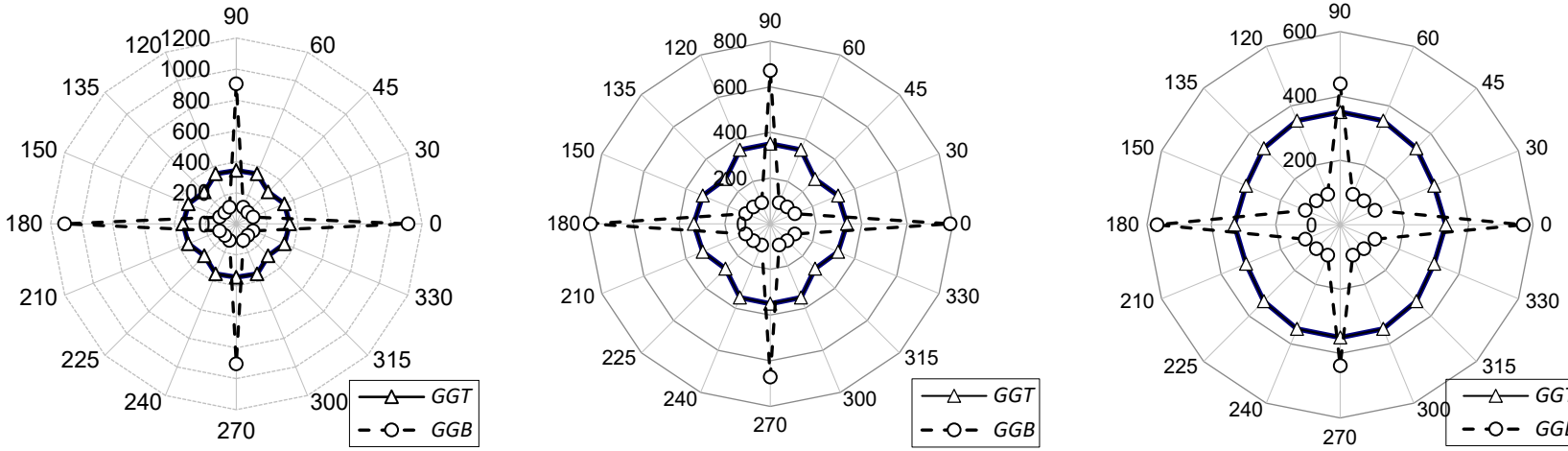

Figure 6. Tensile stiffness of geogrids in kN/m at various strain levels: (a) 0.5 %; (b) 1 %; (c) 2 %.

DEVELOPMENT OF EMPIRICAL EQUATIONS

Empirical equations were developed to estimate the ultimate tensile strength and tensile stiffness for triangular and biaxial geogrids along an arbitrary angle θ. The ultimate tensile strength obtained along this angle, referred herein as $T_{max,\theta}$, can be projected along the cross-machine (CD) and machine (MD) directions to obtain its components along these directions, referred herein as $T_{max,\theta,CD}$ and $T_{max,\theta,MD}$, respectively:

$$T_{max,\theta,CD} = T_{max,\theta} \times \cos\theta \quad (1)$$

$$T_{max,\theta,MD} = T_{max,\theta} \times \sin\theta \quad (2)$$

Then, the contribution factors $\alpha_{CD,\theta}$ and $\alpha_{MD,\theta}$ (in %) of the ultimate tensile strength in CD and MD to the ultimate tensile strengths along θ can be found by dividing $T_{max,\theta,CD}$ and $T_{max,\theta,MD}$ by $T_{max,CD}$ and $T_{max,MD}$, respectively:

$$\alpha_{CD,\theta} = \frac{T_{max,\theta,CD}}{T_{max,CD}} \quad \text{and} \quad \alpha_{MD,\theta} = \frac{T_{max,\theta,MD}}{T_{max,MD}} \quad (3) \text{ \& } (4)$$

Therefore, $T_{max,\theta}$ can be expressed using the contribution factors ($\alpha_{CD,\theta}$ and $\alpha_{MD,\theta}$) and the ultimate tensile strength along CD and MD ($T_{max,CD}$ and $T_{max,MD}$):

$$T_{max,\theta} = \sqrt{(\alpha_{CD,\theta} \times T_{max,CD})^2 + (\alpha_{MD,\theta} \times T_{max,MD})^2} \quad (5)$$

Accordingly, J_θ can also be expressed using the contribution factors obtained for the tensile stiffness ($\beta_{CD,\theta}$ and $\beta_{MD,\theta}$) as follows:

$$J_\theta = \sqrt{(\beta_{CD,\theta} \times J_{CD})^2 + (\beta_{MD,\theta} \times J_{MD})^2} \quad (6)$$

Experimental data obtained in this study was used to estimate the contribution factors α and β (Figures 7 to 10). In these figures, the α and β values (including $\alpha_{CD,\theta}$, $\alpha_{MD,\theta}$, $\beta_{CD,\theta}$ and $\beta_{MD,\theta}$) for each geogrid were considered versus the corresponding angles θ (in degrees). Then, using the least squared error method, the best fit exponential equations were obtained for the factors. It should be noted that the β values were obtained based on the average of the stiffness values at various strain rates for each direction.

The empirical equations obtained using the above explained regression procedure are presented in the plots shown in Figures 7 to 10. The α values obtained from the data presented in Figures 7 and 8 were used in Equation (5) to estimate the ultimate tensile strength along various directions for the triangular and biaxial geogrids reported by Swan and Yuan (2013), Vollmert and Psiorz (2013) and Dong et al. (2010). Specifically, the ultimate tensile strength values that have been reported by these studies in the machine and cross-machine directions were used along with the α values obtained in Figures 7 (for the triangular geogrids) and 8 (for the biaxial geogrid) to estimate the ultimate tensile strength in other directions. The obtained values were then compared to the actual values reported by each study. The results are presented in Figures 11 to 12.

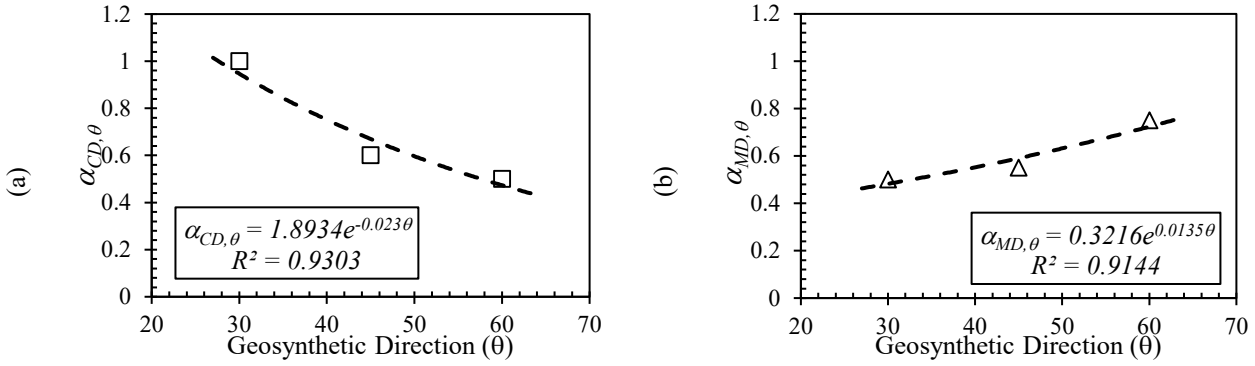

Figure 7. Contribution factors for $T_{max,\theta}$ for the triangular geogrid: (a) CD; (b) MD.

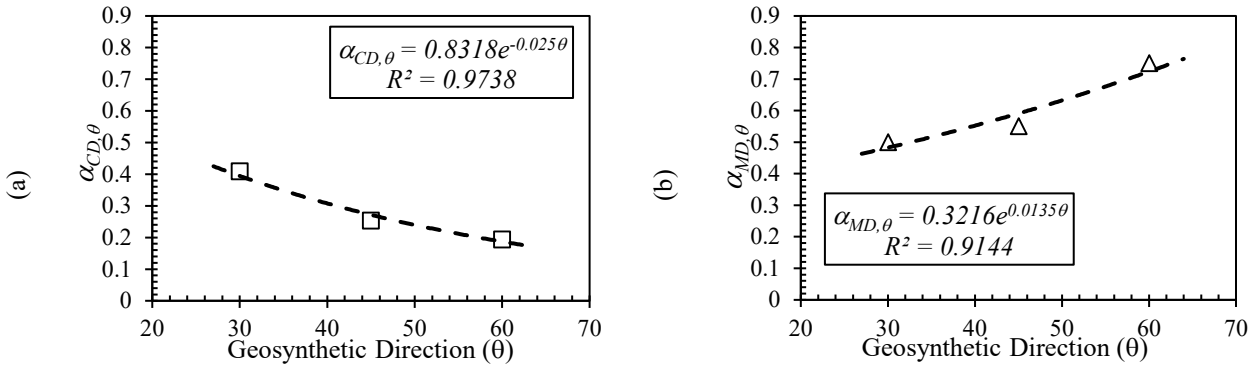

Figure 8. Contribution factors for $T_{max,\theta}$ for the biaxial geogrid: (a) CD; (b) MD.

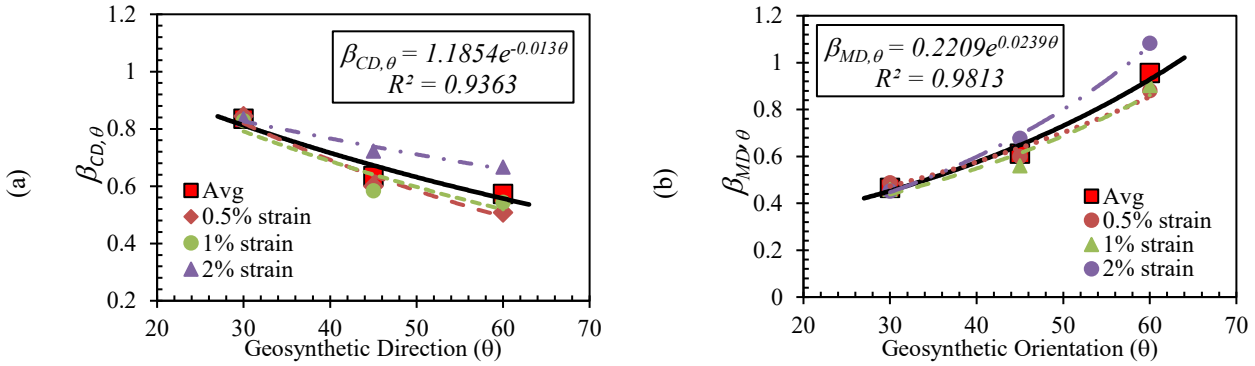

Figure 9. Contribution factors for J_θ for the triangular geogrid: (a) CD; (b) MD.

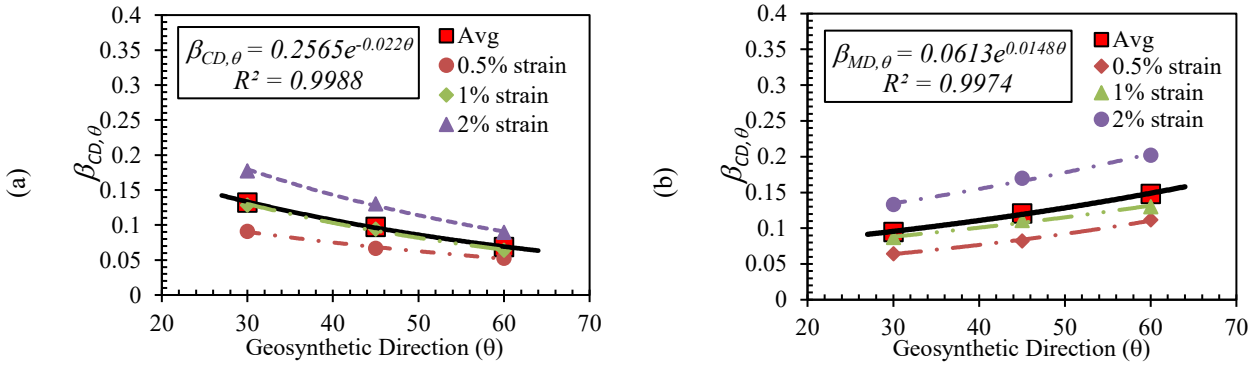

Figure 10. Contribution factors for J_θ for the biaxial geogrid: (a) CD; (b) MD.

Specifically, Figure 11 presents the estimated versus reported ultimate tensile strength for two triangular geogrids reported by Swan and Yuan (2013) and Dong et al. (2010) and Figure 12 presents the estimated versus reported ultimate tensile strength for two biaxial geogrids reported by Vollmert and Psiorz (2013) and Dong et al. (2010). Evaluation of the data presented in Figures 11 and 12, show that the results obtained from the empirical equations matched reasonably well with the numerical and experimental data reported in the original studies.

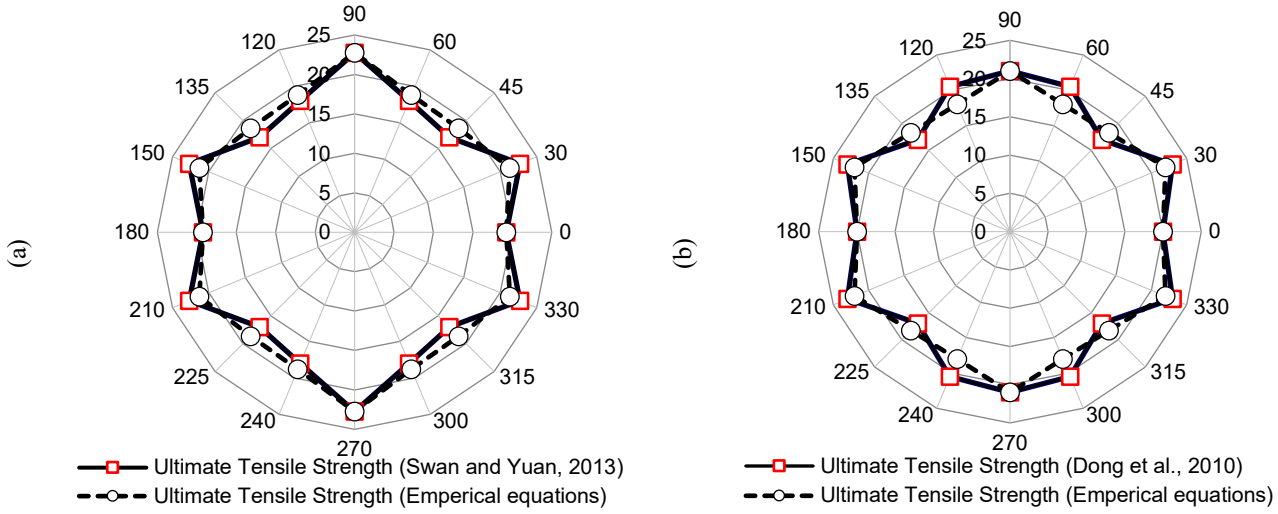

Figure 11. Estimated ultimate tensile strength using empirical equations in this study for the triangular geogrid versus data reported: (a) Swan and Yuan (2013); (b) Dong et al. (2010).

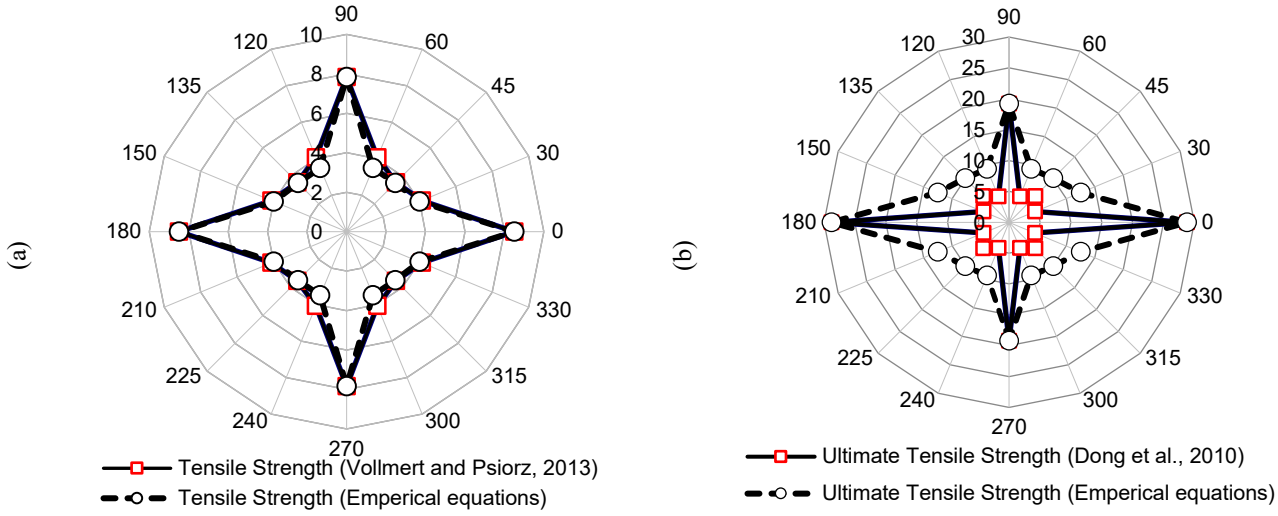

Figure 12. Estimated ultimate tensile strength using empirical equations in this study for the biaxial geogrid versus data reported: (a) Vollmert and Psiorz (2013); (b) Dong et al. (2010).

A similar procedure to that explained above was used to estimate the tensile stiffness. Specifically, the β values obtained from the data presented in Figures 9 and 10 were used in Equation (6) to estimate the tensile stiffness along various directions for the triangular and biaxial geogrids reported by Dong et al. (2010). Specifically, the tensile stiffness values that have been reported by Dong et al. (2010) in the machine and cross-machine directions were used along with

the β values obtained in Figures 9 (for the triangular geogrids) and 10 (for the biaxial geogrid) to estimate the tensile stiffness in other directions. The obtained values were then compared to the actual values reported Dong et al. (2010) as presented in Figure 13. Evaluation of the data presented in Figure 13 shows that the results obtained from the empirical equations matched reasonably well with the numerical results in the original studies.

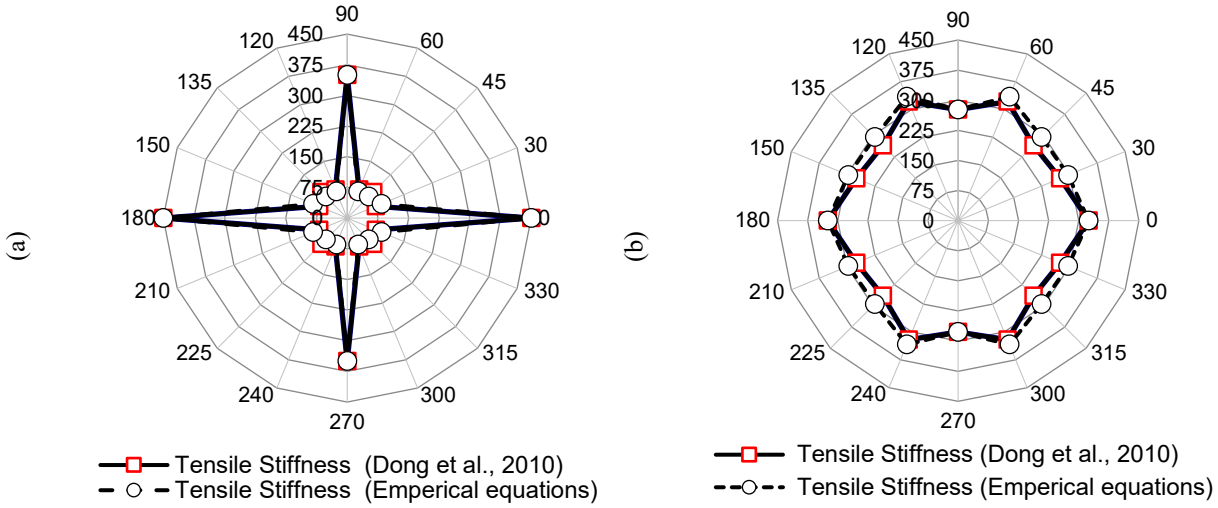

Figure 13. Estimated tensile stiffness using empirical equations in this study versus numerical data reported by Dong et al. (2010): (a) Biaxial geogrid; (b) Triangular geogrid.

SUMMARY AND CONCLUSIONS

The in-isolation properties, including ultimate tensile strength and tensile stiffness, of two types of geogrids, including a biaxial and a triaxial geogrid, were evaluated experimentally along five directions, including the machine and cross-machine directions and at orientations of 30, 45, and 60 degrees between the machine and cross-machine directions. All experiments were conducted using wide-width tensile test equipment.

The ultimate tensile strength and tensile stiffness for the biaxial geogrid were found to be highly dependent on the direction of the tensile load. When the tensile load was applied along the machine or cross-machine directions, the tensile strength and tensile stiffness were comparatively high. However, significantly lower tensile strength and tensile stiffness values were found when the tensile load was applied along other directions.

The ultimate tensile strength and tensile stiffness for the triangular geogrid were found to be similar along all tested directions. This finding suggests that triangular geogrids may provide a comparatively isotropic in-plane mechanical response under different loading conditions.

The experimental data obtained in this study was used to develop empirical equations to estimate the contribution of the ultimate tensile strength in the machine and cross-machine directions to the ultimate tensile strength along an arbitrary angle θ. The contribution factors were used to predict the ultimate tensile strength along various directions of two triangular and two biaxial geogrids reported in the literature. A reasonably good agreement was obtained between the predicted value and the reported value.

Similar to the procedure used for the ultimate tensile strength, the experimental data obtained in this study was used to develop empirical equations to estimate the contribution of the

tensile stiffness in the machine and cross-machine directions to the tensile stiffness along an arbitrary angle θ. The contribution factors were then used to predict the tensile stiffness along various directions of a triangular and a biaxial geogrid reported in the literature. A reasonably good agreement was obtained between the predicted value and the reported value.

It should be noted that the conclusions obtained in this study were based on the observations made in unconfined (in-isolation) conditions. Although the obtained findings may suggest similar isotropic properties for triangular geogrids (and anisotropic properties for biaxial geogrids) in confined conditions, further evaluations are needed to validate in-soil properties of the two types of geogrids.

ACKNOWLEDGEMENT

The first author is grateful for the financial support received from the U.S. Department of State (Fulbright Foreign Student Program). Also, the support received from Tensar Inc. is greatly appreciated.

REFERENCES

Abdullah, C.H. and Edil, T.B. (2007). Behavior of geogrid-reinforced load transfer platforms for embankment on rammed aggregate piers, *Geosynthetics International*, ICE Publishing, 14 (3):141-153.

Abu-Farsakh, M., Chen, Q.M., Sharma, R. and Zhang, X. (2008). Large-scale model footing tests on geogrid-reinforced foundation and marginal embankment soils, *Geotechnical Testing Journal,* ASTM, 31(5):413-423.

ASTM D 6637/D6637M. Standard Test Method for Determining Tensile Properties of Geogrids by the Single or Multi-Rib Tensile Method, *American Society for Testing and Materials*, West Conshohocken, Pennsylvania, USA.

Brown, S.F., Kwan, J. and Thom, N.H. (2007). Identifying the key parameters that influence geogrid reinforcement of railway ballast, *Geotextiles and Geomembranes*, Elsevier, 25(6):326-335.

Dong, Y.L., Han, J. and Bai, X.H. (2010). A numerical study on stress-strain responses of biaxial geogrids under tension at different directions, *GeoFlorida 2010*, ASCE, West Palm Beach, FL, 2551-2560.

Han, J. and Leshchinsky, D. (2010). Analysis of back-to-back mechanically stabilized earth walls, *Geotextiles and Geomembranes,* Elsevier, 28 (3):262-267.

Helstrom, C. L., Humphrey, D.N. and Hayden, S.A. (2006). Geogrid reinforced pavement structure in a cold region, *13th International Conference on Cold Regions Engineering: Current Practices in Cold Regions Engineering*, Orono, ME, 57-69.

Koerner, R. M. (2012). *Designing with Geosynthetics*, 6th ed., Pearson Prentice Hall, Upper Saddle River, NJ, USA.

Swan, Jr., R.H. and Yuan, Z. (2013). Tensile behavior of triaxial geogrid: Application of the theoretical method, *Geosynthetics 2013*, IFAI, Long Beach, CA, 424-433.

Tang, X.C., Chehab, G.R. and Palomino, A. (2008). Evaluation of geogrids for stabilizing weak pavement subgrade, *International Journal of Pavement Engineering,* Taylor and Francis, 9(6):413-429.

Vollmert, L. and Psiorz, C. (2013). Stabilization of unbound granular layers – reinforcement required, *Geotechnics Special ICSMGE*, 09/2013 (Special Edition for 18th ICSMGE, Paris, 2013).